Histochem Cell Biol (2005) 123: 501–512
DOI 10.1007/s00418-005-0753-x

ORIGINAL PAPER

**Toshiyuki Matsuzaki · Natsuko Machida · Yuki Tajika
Abdushukur Ablimit · Takeshi Suzuki · Takeo Aoki
Haruo Hagiwara · Kuniaki Takata**

Expression and immunolocalization of water-channel aquaporins in the rat and mouse mammary gland

Accepted: 14 December 2004 / Published online: 21 April 2005

Abstract We examined the expression and immunolocalization of water-channel aquaporins in the mammary gland by reverse transcriptase polymerase chain reaction (RT-PCR), immunoblotting, and immunohistochemistry. RT-PCR and immunoblotting revealed the expression of aquaporin-1 (AQP1) and AQP3 in the lactating rat mammary gland. AQP3 was detected in the alveolar epithelium and duct system whereas AQP1 was found in the capillaries and venules. AQP3 was present in the basolateral membrane of secretory epithelial cells and intralobular and interlobular duct epithelial cells. The main duct near the orifice in the nipple, which is comprised of a stratified epithelium, bore AQP3 in its basal and intermediate layers. AQP1 was located in both the apical and basolateral membranes of capillary and venule endothelia. AQP3 was not detected in virgin females. AQP3 was found in some differentiating mammary epithelial cells in the pregnant rat. AQP1 was present in capillaries and venules in the differentiating mammary gland of the pregnant rat and in the mammary fat pad of virgin females. We found a similar distribution of AQP1 and AQP3 in the mouse. AQP1 and AQP3 seem to play roles in the synthesis and/or secretion of milk.

Keywords Water channel · Aquaporin · AQP · Mammary gland · Immunohistochemistry

T. Matsuzaki (✉) · N. Machida · Y. Tajika · A. Ablimit
T. Suzuki · T. Aoki · H. Hagiwara · K. Takata
Department of Anatomy and Cell Biology,
Gunma University Graduate School of Medicine,
Showa-machi 3-39-22, Maebashi,
Gunma 371-8511, Japan
E-mail: matoshi@med.gunma-u.ac.jp
Tel.: +81-27-2207902
Fax: +81-27-2207906

Introduction

Cells are surrounded by a plasma membrane comprised of a lipid bilayer that separates the intracellular compartment from the extracellular compartment and maintains a suitable intracellular environment. Water can permeate the plasma membrane by simple diffusion; however, bulk water flow is mediated by the channel machinery. The first water channel was identified in the erythrocyte as an integral membrane protein copurified with the erythrocyte Rh(D) antigen and originally named CHIP28 (channel-like integral protein of 28 kDa) (Smith et al. 1991). By expressing CHIP28 in *Xenopus* oocytes, Preston et al. (1992) showed that CHIP28 is a water-channel molecule. Fushimi et al. (1993) isolated another isoform of water channels in the renal collecting duct (WCH-CD) with the homology cloning method. Agre et al. (1993) coined the name aquaporin for water-channel proteins. CHIP28 and WCH-CD were termed aquaporin-1 (AQP1) and AQP2, respectively, thereafter. At present, at least eleven aquaporin isoforms (AQP0–AQP10) have been identified in mammals (for review, see Takata et al. 2004). Some aquaporins, such as AQP3, AQP7, and AQP9, show permeability to glycerol as well as water and are termed aquaglyceroporins. AQP1, AQP2, AQP4, and AQP5 are selectively permeable by water and are classified as aquaporins in a narrow sense (for review, see Agre et al. 2002). They are widely distributed in water-handling organs and tissues. In the kidney, at least six isoforms, AQP1, AQP2, AQP3, AQP4, AQP6, and AQP7, are expressed, and each plays an important role in water reabsorption (for review, see Nielsen et al. 2002). In gland tissues such as the salivary gland, lacrimal gland, sweat gland, pyloric gland, and duodenal gland, AQP5 is present in apical membranes of acinar secretory cells and seems to play a role in secretion (Matsuzaki et al. 1999a, 2003; Nejsum et al. 2002; Song et al. 2002).

The mammary gland produces and secretes milk comprised of water, lipid, sugar, proteins, and so on (for

review, see Shennan and Peaker 2000). Since aquaporins are expressed in gland tissues, we examined whether an aquaporin is expressed in the mammary gland by reverse transcriptase polymerase chain reaction (RT-PCR), immunoblotting, and immunohistochemistry in the rat and the mouse.

Materials and methods

Antibodies

The oligopeptide TM31 corresponding to amino acids 234–247 of rat/mouse AQP1 (CRSSDFTDRMKVWTS; N-terminal cysteine residue was added for conjugation) (Zhang et al. 1993) was synthesized with a Model 431A peptide synthesizer (Applied Biosystems, Foster, CA, USA). Rabbit polyclonal antibodies to rat/mouse AQP1 (RaTM31) and guinea pig polyclonal antibodies to rat/mouse AQP1 (GPTM31) were raised by using the TM31 peptide conjugated to keyhole limpet hemocyanin (Pierce, Rockford, IL, USA). Rabbit polyclonal antibodies to rat AQP3 (RaTM5) have been characterized previously (Matsuzaki et al. 1999b). Guinea pig polyclonal antibodies to rat AQP3 (GPTM5b) were raised with the use of the same immunogen as for RaTM5. Affinity purification of the antibodies was carried out using SulfoLink coupling gel (Pierce) or Affi-Gel 10 (Bio-Rad Laboratories, Hercules, CA, USA) and yielded affinity-purified RaTM31 (AffRaTM31), affinity-purified GPTM31 (AffGPTM31), affinity-purified RaTM5 (AffRaTM5), and affinity-purified GPTM5b (AffGPTM5b). Guinea pig polyclonal antibodies to the sugar transporter GLUT1 have been described previously (Shin et al. 1996).

Animals and tissue preparation

All animal experiments were in compliance with the National Institutes of Health (NIH) Guide for the Care and Use of Laboratory Animals and approved by the Animal Care and Experimentation Committee, Gunma University, Showa Campus (admission no. 30067, 40020). Wistar rats were obtained from Japan SLC (Shizuoka, Japan) and the Institute of Experimental Animal Research, Gunma University Graduate School of Medicine, and maintained on normal chow. BALB/c mice were obtained from Japan SLC and maintained on normal chow. Virgin female rats aged 6 and 12 weeks were used. A pregnant rat was used on day 17 post coitum. Lactating rats were used on days 6 and 8 post partum. Lactating mice were used on days 7 and 17 post partum. Animals were deeply anesthetized with an intraperitoneal injection of sodium pentobarbital and killed by cervical dislocation. Rat tissues, such as the kidney, submandibular gland, and testis, were obtained from 6-week-old male Wistar rats for RT-PCR and immunoblotting. Mouse kidney was obtained from 6-week-old male BALB/c mice.

Reverse transcriptase polymerase chain reaction

Tissues were quickly removed and frozen in liquid nitrogen prior to use. Total RNA was isolated with the use of an RNeasy Mini Kit (Qiagen, Valencia, CA, USA), reverse-transcribed using a ReverTraAce-alpha-Kit (Toyobo, Osaka, Japan), and amplified by PCR with KOD-Plus-DNA polymerase (Toyobo). The PCR primers (Table 1) were designed to amplify the entire open reading frame of each rat aquaporin isoform. PCR was performed for 30 cycles of denaturation at 94°C for 1 min, annealing at 60°C for 1.5 min, and elongation at 68°C for 2 min. A final extension at 68°C for 5 min was done. Equal volumes of PCR products from each sample were separated by electrophoresis on a 2% agarose gel and visualized by staining with ethidium bromide. Amplification products of the expected sizes were purified from the gel and subjected to fluorescent sequencing with an ABI PRISM 3100 genetic analyzer (Applied Biosystems).

Immunoblotting

Tissues were quickly removed and frozen in liquid nitrogen prior to use. Tissue homogenates were prepared with a glass homogenizer in phosphate-buffered saline containing 5 μg/ml leupeptin, 5 μg/ml aprotinin, 5 μg/ml pepstatin, 5 mM EDTA, and 2 mM phenylmethylsulfonyl fluoride. Treatment with glycosidase was performed using *N*-Glycosidase F (Roche Diagnostics, Mannheim, Germany), according to the manufacturer's directions, at 37°C overnight. These samples were denatured in an equal volume of buffer containing 50 mM Tris-HCl, pH7.5, 4%SDS, 300 mM dithiothreitol, and 50% glycerol at 37°C for 30 min, subjected to SDS-polyacrylamide gel electrophoresis, and transferred onto polyvinylidene difluoride membranes with standard methods. Membranes were incubated with antibodies to AQP1 or AQP3 at 4°C overnight followed by horseradish-peroxidase-coupled secondary antibodies (DAKO, Glostrup, Denmark) at room temperature for 1–3 h. The visualization was performed using ECL plus (Amersham Biosciences Pharmacia, Buckinghamshire, UK) and Hyperfilm ECL (Amersham Biosciences).

Immunohistochemistry

Tissues were quickly removed from the animals, immediately embedded in Tissue-Tek OCT compound (Sakura Finetechnical, Tokyo, Japan), frozen in liquid nitrogen, and stored at −80°C prior to use. Some tissues were quickly removed and fixed with 3% paraformaldehyde-PBS for 1–3 h on ice. Fixed tissues for cryostat sections were immersed in 20% sucrose-PBS,

Table 1 Sequence of specific sets of primers used in reverse transcriptase polymerase chain reaction (RT-PCR) analyses

Aquaporin isoforms		Primer sequences 5′ to 3′	Product size, bp	GenBank Accession no.
AQP1	Forward	5′-TACAAGCTTGCATGGCCAGCGAAATCAAGAAGAAGCTCTTCTGGAGGGCTGTG-3′	830	X70257
	Reverse	5′-CGCGGATCCCTATTTGGGCTTCATCTCCACCCTGGAGTTGATATCATCAGCAT-3′		
AQP2	Forward	5′-CGCGCAAGCTTGCATGTGGGAACTCAGATCCATAGCCTTCTCCGAGCAGTGCTGGCT-3′	838	D13906
	Reverse	5′-ATAGGATCCTCAGGCCTTGCTGCCGCGAGGCAGGCTCTGAGGAGAGTGGAGCTCCA-3′		
AQP3	Forward	5′-TTAATAAGCTTTGATGAACCGTTGCGGGGAGATGCTCCACATCCGCTACCGGCTGCTT-3′	879	D17695
	Reverse	5′-AAGGATCCTCAGATCTGCTCCTTGTGCTTCATGTGGGCCAGCTTCACATTCTCTGCCT-3′		
AQP4	Forward	5′-CTAAAGCTTTAATGAGTGACGGAGCTGCAGCGAGGCGGTGGGGTAAGTGTGGA-3′	992	U14007
	Reverse	5′-CGCGAATTCTCATACAGAAGATAATACCTCTCCAGACGAGTCCTTCCCCTTCT-3′		
AQP5	Forward	5′-AGCTCAAGCTTCCATGAAAAAGGAGGTGTGCTCCCTTGCCTTCTTCAAGGCGGTGTTTC-3′	819	U16245
	Reverse	5′-AAGGATCCTCAGTGTGCCGTCAGCTCGATGGTCTTCTTCCTCTCCTCGATGATCTT-3′		
AQP6	Forward	5′-CTAAAGCTTGCATGGAGCCTGGGCTGTGTAACAGGGCTTACCTGCTGGTTGGC-3′	801	NM_022181
	Reverse	5′-CGCGAATTCTTACACGCTCACTTCTGTGTCCTCTGAGTTCGTCTGTGATTCTT-3′		
AQP7	Forward	5′-CGCAAGCTTGCATGGCCGGTTCTGTGCTGGAGAACATACAATCAGTGCTACAG-3′	830	AB000507
	Reverse	5′-ATAGGATCCCTAAGAACCCTGTGGTGGTATGCCGGCGTGAATTAAGCCCAGGT-3′		
AQP8	Forward	5′-TACAAGCTTACATGTCTGGGGAGCAGACGCCGATGTGTAGTATGGACCTACGT-3′	812	AB005547
	Reverse	5′-CGCGGATCCTCACCTCGACTTTAGAATCAGGCGGGTTTTCTCATCTCCAATGA-3′		
AQP9	Forward	5′-TACAAGCTTACATGCCTTCTGAGAAGGACGGTGCCAAGAAGAGCCTCATGCAG-3′	908	NM_022960
	Reverse	5′-CGCGGATCCCTACATGATGACACTGAGCTCGTGTTTCTCTAGGTTGTTCTCAG-3′		

embedded in Tissue-Tek OCT compound, frozen in liquid nitrogen, and stored at −80°C. Fixed tissues for semithin frozen sections were immersed in 2.3 M sucrose–0.1 M sodium phosphate buffer, pH7.4, and frozen in liquid nitrogen.

Cryostat sections 7-to-10-μm thick or semithin frozen sections 1-to-1.5-μm thick were mounted on poly-L-lysine-coated glass slides. Sections from unfixed tissues were immediately fixed in ethanol or acetone at −20°C for 30 min and rinsed with PBS. Sections from paraformaldehyde-fixed tissues were treated with ethanol or acetone at −20°C for 30 min or not and rinsed with PBS. Indirect immunofluorescence staining was performed essentially as described (Matsuzaki et al. 1999a). Fluorescently labeled secondary antibodies used were: (1) Rhodamine Red-X-conjugated donkey antibodies to rabbit IgG, (2) Rhodamine Red-X-conjugated donkey antibodies to guinea pig IgG, (3) fluorescein isothiocyanate (FITC)-conjugated donkey antibodies to rabbit IgG, and (4) FITC-conjugated donkey antibodies to guinea pig IgG. All these secondary antibodies were purchased from Jackson Immunoresearch (West Grove, PA, USA). For nuclear counterstaining, we used 4′,6-diamidino-2-phenylindole (DAPI) for conventional fluorescence microscopy and SYBR Green I or TO-PRO-3 for laser confocal microscopy. To stain F-actins, we used fluorescein-labeled phalloidin (Molecular Probes, Eugene, OR, USA). The specificity of AQP1and AQP3 immunostaining was verified by preincubating the antibodies with the peptide (10–50 μg/ml) used as the immunogen. The specimens were examined with a BX-62 microscope equipped with Nomarski differential interference-contrast and epifluorescence optics (Olympus, Tokyo, Japan) or an Axioplan 2 microscope (Carl Zeiss, Jena, Germany) equipped with an MRC-1024ES laser confocal system (Bio-Rad Laboratories).

Results

Reverse transcriptase polymerase chain reaction

RT-PCR was performed in the mammary gland and control tissues (Fig. 1). AQP1, AQP2, AQP3, AQP4, AQP6, and AQP7 were amplified in the kidney; AQP5 was amplified in the submandibular gland; and AQP8 and AQP9 were amplified in the testis, as described previously (for review, see Takata et al. 2004). In the lactating rat mammary gland, strong bands of AQP1 and AQP3 were observed. A relatively clear band for AQP7 and very weak bands for AQP4, AQP5, and AQP9 were also observed in the mammary gland. We also checked the nucleotide sequences of these PCR products and confirmed the results. Based on the results of RT-PCR, we performed immunoblotting and immunohistochemistry in the mammary gland with antibodies to AQP1 and AQP3.

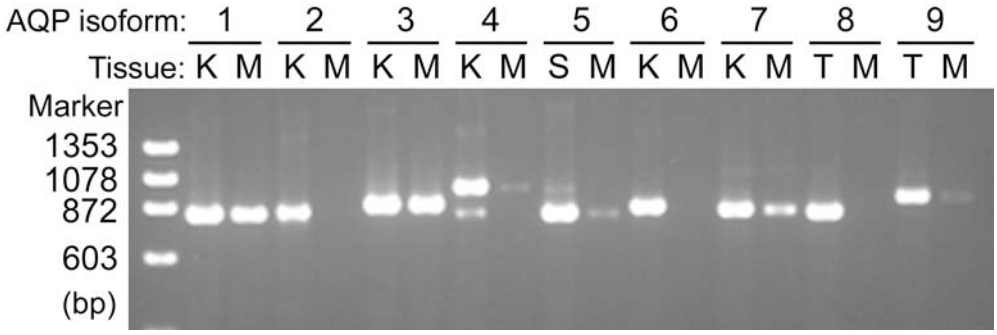

Fig. 1 Reverse transcriptase polymerase chain reaction (RT-PCR) for aquaporins in the lactating rat mammary gland. Mammary gland (*M*) was obtained from the lactating rat on day 8 post partum. Kidney (*K*), submandibular gland (*S*), and testis (*T*) from 6-week-old male rats were used as positive controls. Total RNA (200 ng) was reverse transcribed and amplified by PCR with specific primer pairs for each rat aquaporin isoform shown in Table 1. Equal volumes of PCR products from each sample were separated by electrophoresis on a 2% agarose gel and visualized by staining with ethidium bromide. Strong bands for aquaporin-1 (AQP1) and AQP3, a relatively clear band for AQP7, and faint bands for AQP4, AQP5, and AQP9, are seen

Immunoblotting

Aquaporin-1

Homogenates from the rat kidney and lactating rat mammary gland were electrophoresed and subjected to immunoblotting with antibodies to AQP1 (AffRaTM31) (Fig. 2A). Two bands were detected in the kidney, as described previously (Sabolić et al. 1992). The digestion with *N*-glycosidase F clearly showed that the higher molecular weight band corresponds to the glycosylated form of AQP1. In the mammary gland, only the lower molecular weight band was detected. This band remained after glycosidase treatment.

Aquaporin-3

Homogenates were electrophoresed and subjected to immunoblotting with antibodies to AQP3 (AffRaTM5) (Fig. 2A). Two bands were detected in both the kidney and mammary gland, as described previously (Ishibashi et al. 1997; Matsuzaki et al. 1999b). Digestion with *N*-glycosidase F clearly showed that the higher molecular weight band corresponds to the glycosylated form of AQP3. The difference in the apparent molecular weight of the glycosylated forms in the kidney and mammary gland suggests a tissue-specific glycosylation of AQP3. The lower molecular weight band remained after glycosidase treatment.

Specificity of the antibodies

When we used guinea pig antibodies, namely AffGPTM31 and AffGPTM5b, the same band patterns were observed in the kidney and mammary gland (Fig. 2B). The bands, detected by AffRaTM31, AffRaTM5, AffGPTM31, and AffGPTM5b, disappeared when antibodies were preincubated with the corresponding antigen peptide(Fig. 2A, B). These results demonstrated the specificity of the antibodies and the presence of both AQP1 and AQP3 proteins in the lactating rat mammary gland.

Immunohistochemistry in the rat mammary gland

We examined mammary glands in the lactating phase from lactating rats on days 6 and 8 post partum, resting phase from virgin female rats of age 6 and 12 weeks, and in the pregnant phase from a pregnant rat on day 17 post coitum.

Aquaporin-3

We first examined the cryostat sections of the lactating mammary gland at lower magnification. Labeling for AQP3 was present in alveoli and ducts (Fig. 3A, B). The intensity of the labeling was not uniform, with some alveoli intensely labeled and others weakly labeled. When alveoli were examined at a higher magnification, AQP3 was found to localize to the basolateral side of secretory cells. Observations of both cryostat sections by laser confocal microscopy and semithin frozen sections by conventional fluorescence microscopy clearly showed that AQP3 was restricted to the basolateral membrane (Fig. 3E–G). To examine whether myoepithelial cells bear AQP3, we performed F-actin staining with fluorescently labeled phalloidin that intensely labels myoepithelial cells. Double labeling for AQP3 and F-actin clearly demonstrated that labeling for AQP3 was restricted to secretory epithelial cells and absent in myoepithelial cells (Fig. 3H–J). Further, we performed double labeling for AQP3 and the sugar transporter GLUT1 that is present in basolateral membranes of secretory epithelial cells (Takata et al. 1997). AQP3 was colocalized with GLUT1, demonstrating that AQP3 was restricted to the basolateral membrane of secretory cells (Fig. 3K, L).

AQP3 was also present in the duct system, and we carefully examined its distribution. The labeling intensity for AQP3 was not uniform among the ducts. AQP3 was present in most of the intralobular and interlobular ducts where it was distributed in the basolateral mem-

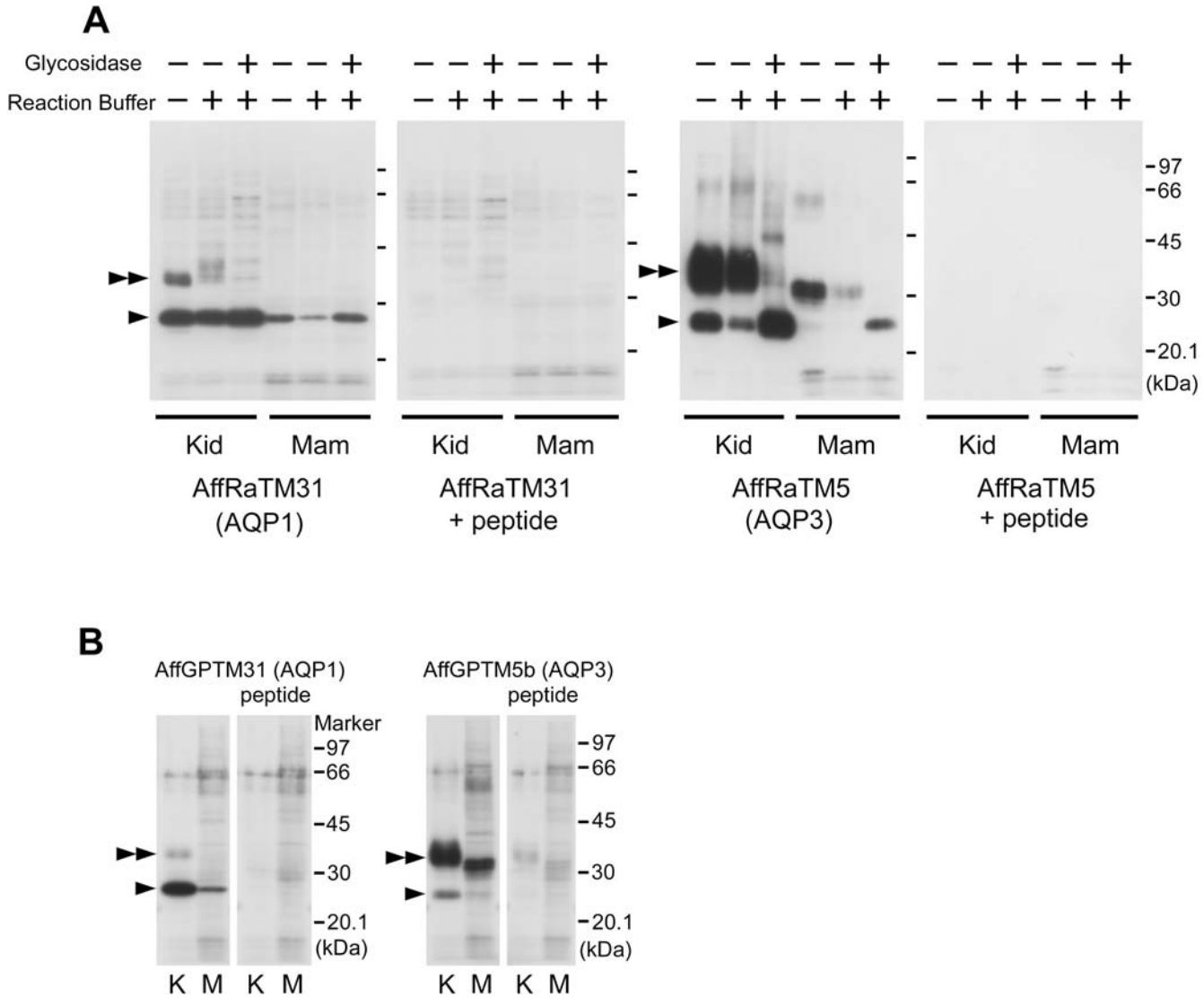

Fig. 2 Immunoblotting of the lactating rat mammary gland with antibodies to aquaporin-1 (AQP1) and AQP3. **A** Six micrograms of rat kidney homogenate (*Kid*) and 3 μg of rat kidney papilla homogenate (*Kid*) for AQP1 and AQP3 analysis, respectively, and 15 μg of mammary gland homogenate (*Mam*) from the lactating rat on day 8 post partum with or without *N*-glycosidase F treatment were subjected to immunoblotting with rabbit antibodies AffRaTM31 (AQP1; 33 ng/ml) and AffRaTM5 (AQP3; 60 ng/ml). Upper bands (*double arrowheads*) and lower bands (*arrowheads*) are derived from glycosylated and unglycosylated forms of AQP1 and AQP3. These bands completely disappear in the presence of the antigen peptide TM31 (2 μg/ml) or TM5 (20 μg/ml). **B** Five micrograms of rat kidney homogenate (*K*) and 30 μg of mammary gland homogenate (*M*) from the lactating rat on day 8 post partum were subjected to immunoblotting with antibodies AffGPTM31 (AQP1; 60 ng/ml) and AffGPTM5b (AQP3; 60 ng/ml). Upper bands (*double arrowheads*) and lower bands (*arrowheads*) are observed in AQP1 and AQP3, as seen in **A**. These bands completely disappear in the presence of the antigen peptides TM31 (1 μg/ml) or TM5 (2 μg/ml)

brane of a simple epithelium. The main duct is lined by a stratified cuboidal-columnar epithelium. Some regions of the main duct were strongly labeled whereas others were labeled weakly or not at all (Fig. 4A, C). In the positive regions, labeling for AQP3 was restricted to the cell membrane of the basal-to-intermediate layers and absent in the surface layer (Fig. 4A, D). The stratified cuboidal-columnar epithelium changes to a stratified squamous epithelium near the orifice at the surface of the nipple where the labeling intensity abruptly increased and AQP3 was detected in the cell membrane of basal and intermediate layers (Fig. 4A, B). Labeling for AQP3 was evident throughout the epidermis of the nipple and body surface (Figs. 4A, 5A), as described previously (Matsuzaki et al. 1999b).

We then compared the expression of AQP3 in the resting phase and the pregnant phase. In the resting phase, epithelial ducts infiltrated a mammary fat pad comprised of adipose tissue. No labeling for AQP3 was seen although AQP3 in epidermis, hair follicles, and sebaceous glands was properly labeled (Fig. 5A, B), as described previously (Matsuzaki et al. 1999b) In the pregnant phase, immature lobuli showed proliferation within the fat pad, with AQP3 mainly expressed at the periphery (Fig. 5C). Higher magnification views showed

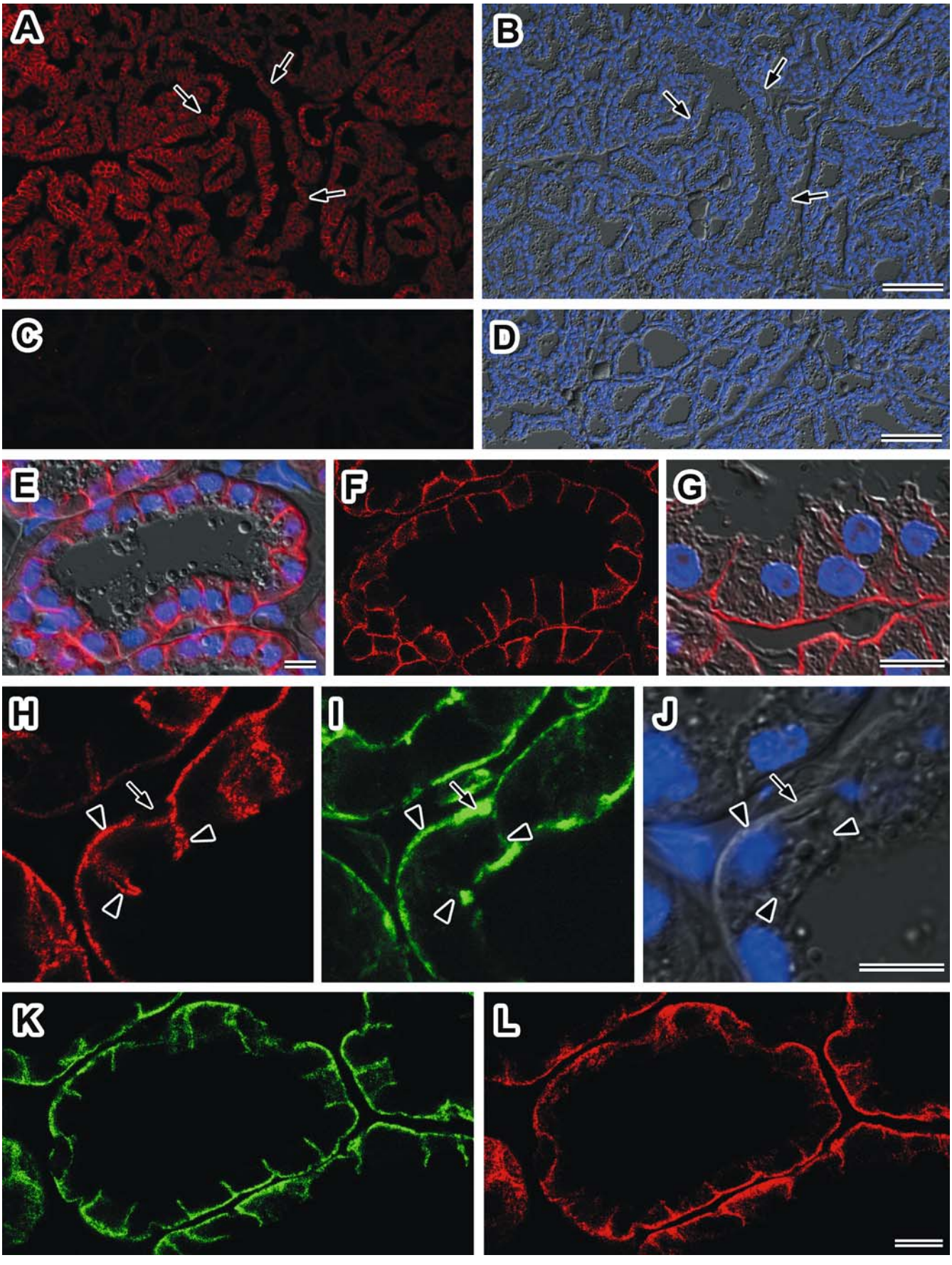
A
B
C
D
E
F
G
H
I
J
K
L

◀

Fig. 3 Immunofluorescence microscopy of aquaporin-3 (AQP3) in the lactating rat mammary gland. Cryostat sections (**A–F, H–I**) and a semithin frozen section (**G**) were stained. AQP3 detected by the use of AffRaTM5 (**A, C, E, F, H**) or GPTM5b (**G**) was labeled with Rhodamine Red-X (*red*). Nuclei were counterstained with DAPI (*blue*). **A–D** Lower magnification views: Fluorescence images for AQP3 (**A, C**) and corresponding Nomarski differential interference-contrast images merged with DAPI fluorescence images (**B, D**). **A, B** Labeling for AQP3 is present in alveoli and ducts (*arrows*). **C, D** A section was incubated with AffRaTM5 in the presence of TM5 peptide (50 μg/ml) used as an immunogen. No labeling is seen. Bars, 100 μm. **E–G** Higher magnification views of the alveolar secretory epithelium: Conventional fluorescence microscopic images for AQP3 and nuclei merged with Nomarski images (**E, G**) and a confocal image for AQP3 in the area corresponding to that in **E** (**F**). Labeling for AQP3 is present in the basolateral membrane but absent in the apical membrane or in the cytoplasm. Bars, 10 μm. **H–J** A higher magnification view of the basal side of the secretory epithelial cell: F-actin was stained with fluorescein-labeled phalloidin (*green*). Projection images of consecutive 8-slice confocal images at 0.3-μm intervals for AQP3 (**H**) and F-actin (**I**) and a corresponding Nomarski image with a DAPI image (**J**). Labeling for AQP3 is restricted to the basolateral membrane of the secretory epithelial cell (*arrowheads*) and absent in the myoepithelial cell intensely labeled with phalloidin (*arrow*). Bar, 10 μm. **K, I** AQP3 and GLUT1 were double stained with rabbit antibodies to AQP3 (RaTM5) labeled with FITC (*green*) and guinea pig antibodies to GLUT1 labeled with Rhodamine Red-X (*red*). Projection images of consecutive 3-slice confocal images at 1-μm intervals for AQP3 (**K**) and GLUT1 (**I**) in the lobuli. Labeling for AQP3 and GLUT1 is colocalized to the basolateral membrane of the secretory epithelial cell. Bar, 10 μm

restricted labeling for AQP3 in the basal and lateral sides (Fig. 5C).

Aquaporin-1

In the lactating mammary gland, prominent labeling for AQP1 was scattered in the stroma but not in the alveolar epithelia or duct systems (Fig. 6A). Higher magnification views showed that AQP1 was present in capillaries, as described previously (Nielsen et al. 1993), and venules (Fig. 6C). Semithin frozen sections clearly demonstrated that the labeling for AQP1 was located in both the apical and basolateral membranes of endothelial cells (Fig. 6D, E).

In the resting phase, some labeling for AQP1 was seen in capillaries and small vessels in the mammary fat pad (Fig. 7A). In the mammary gland of the pregnant rat, extensive labeling was seen in capillaries and small vessels within the differentiating immature lobuli (Fig. 7B).

Histochemical controls

The specificity of AQP3 and AQP1 labeling was confirmed by replacing the antibodies to AQP3 and AQP1 with a mixture of antibodies preincubated with each antigen peptide. No specific labeling was seen (Figs. 3C, D, 6B). All the antibodies to AQP3, namely, RaTM5, AffRaTM5, GPTM5b, and AffGPTM5b; and the antibodies to AQP1, namely, RaTM31, AffRaTM31, GPTM31, and AffGPTM31; gave the same results.

Other aquaporin isoforms

We also generated specific antibodies to AQP2 (Tajika et al. 2002), AQP4, AQP5 (Matsuzaki et al. 1999a), AQP6, AQP7, and AQP9. When the immunohistochemistry was performed using these antibodies, no specific labeling was detected in the lactating rat mammary gland (data not shown).

Immunohistochemistry in the mouse mammary gland

Antibodies to AQP1 were generated against the sequence common to rat and mouse AQP1. Antibodies to AQP3 were generated against the rat AQP3 sequence. There is only one amino acid change in the mouse (EEENVKLAHMKHKEQI) (Ma et al. 2000) compared with the corresponding rat sequence (EAENVKLAHMKHKEQI). We confirmed that antibodies to rat AQP3 also recognize the mouse AQP3 in the mouse kidney by immunoblotting and immunohistochemistry (data not shown).

We also examined the distribution of AQP1 and AQP3 in the lactating mouse mammary gland (Fig. 8). Labeling for AQP1 was present in the capillaries and small vessels, as seen in the rat mammary gland. Labeling for AQP3 was restricted to the basolateral membrane of alveolar secretory cells. Although the localization was the same as in the rat mammary gland, the labeling intensity for AQP3 was weaker in the mouse than the rat. The labeling for AQP1 and AQP3 completely disappeared in the presence of each antigen peptide (data not shown).

Discussion

We showed that the lactating rat mammary gland expresses the water-channel proteins AQP1 and AQP3, by RT-PCR, immunoblotting, and immunohistochemistry. AQP1 is present in endothelial cells of the capillaries and venules where it is located in both the apical and basolateral membranes. AQP1 is a water-selective channel and seems to play a role in the transcellular transfer of water from the blood to the interstitial space.

In alveolar secretory epithelia, AQP3 is localized to the basolateral membrane. Labeling for AQP3 differs in intensity among alveoli, which might be caused by the different state of the alveolar secretory cells, namely, synthetic or secretory. AQP3 is absent in the epithelial duct of the virgin female rat, and a small amount of AQP3 is present in the pregnant rat. AQP3 seems to be expressed upon the differentiation of alveolar secretory cells.

We carefully examined the distribution of AQP3 in the duct system. Some ducts expressed an abundance of

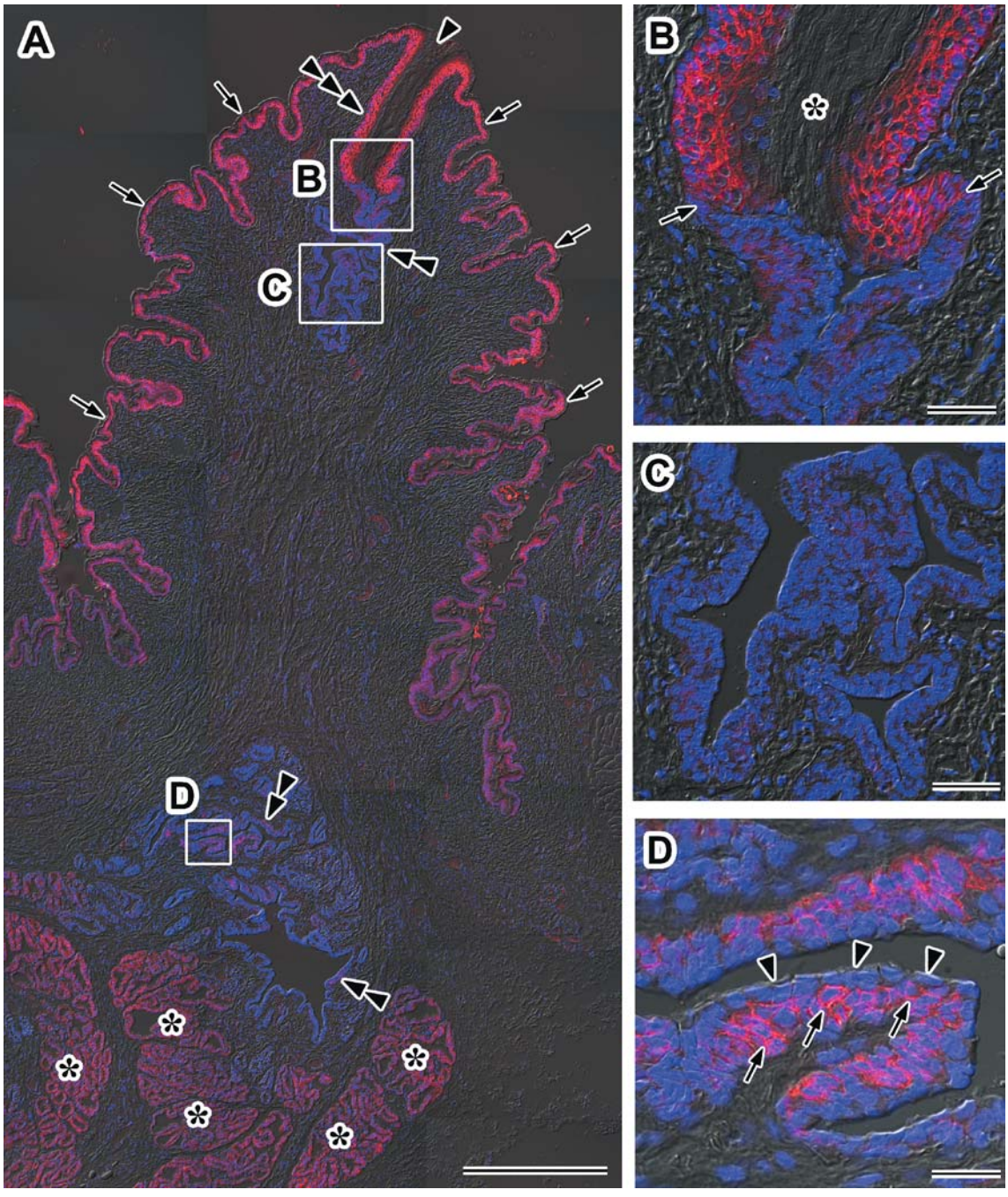

Fig. 4 Distribution of aquaporin-3 (AQP3) in the duct system of the lactating rat mammary gland. A cryostat section was stained. AQP3 detected by the use of AffRaTM5 was labeled with Rhodamine Red-X (*red*). Nuclei were counterstained with DAPI (*blue*). Fluorescence images for AQP3 and nuclei merged with corresponding Nomarski images are shown. A lower magnification view around the nipple (**A**). Higher magnification views of areas **B–D** indicated by *rectangles* are shown in right panels. **A** Labeling for AQP3 is present in some regions along the main duct (*double arrowheads*) as well as alveoli (*asterisks*). The main duct near the orifice at the surface of the nipple (*triple arrowhead*) and epidermis of the skin (*arrows*) bear strong labeling for AQP3. An *arrowhead* indicates the orifice of the main duct. **B** Labeling intensity for AQP3 abruptly increases at the region pointed to by *arrows* where the stratified cuboidal-columnar epithelium changes to a cornified stratified squamous epithelium. An *asterisk* indicates the cornified layer. **C** There is little labeling for AQP3 in this region. **D** Labeling for AQP3 is localized to the cell membrane of the basal and intermediate layers of the stratified cuboidal-columnar epithelium (*arrows*). No labeling is seen in the surface layer (*arrowheads*). Bar in **A**, 500 μm. Bars in **B–D**, 50 μm

AQP3 and others expressed little or no AQP3. There seems to be no relation between the expression level of AQP3 and the position of the duct, namely, whether the duct is intralobular, interlobular, or a main duct. The significance of this differential expression level remains unclear.

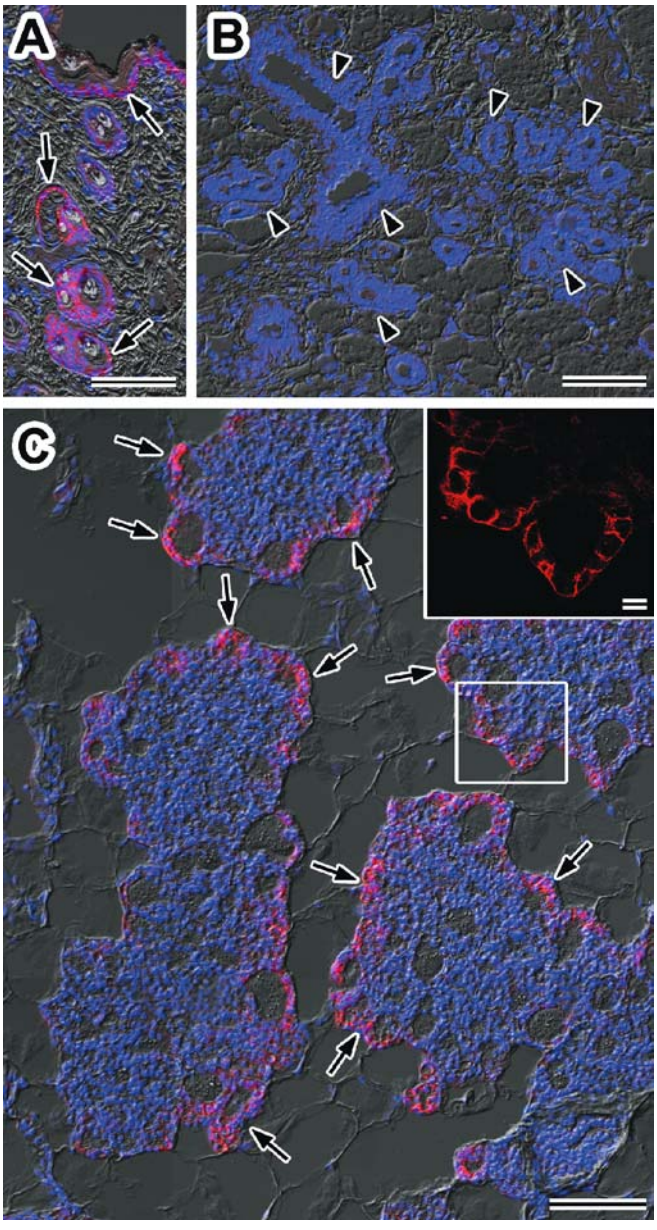

Fig. 5 Changes in the expression of aquaporin-3 (AQP3) during development. Resting-phase mammary gland from a 6-week-old virgin female rat (**A, B**) and pregnant-phase mammary gland from a pregnant rat on day 17 post coitum (**C**). Cryostat sections were stained. AQP3 detected by the use of RaTM5 was labeled with Rhodamine Red-X (*red*). Nuclei were counterstained with DAPI (*blue*). Fluorescence images for AQP3 and nuclei merged with corresponding Nomarski images are shown. **A, B** Epithelial ducts infiltrate through a mammary fat pad. No labeling for AQP3 is seen (*arrowheads* in **B**) although AQP3 in the epidermis, hair follicle, and sebaceous gland is properly labeled (*arrows* in **A**) in the same section. **C** Differentiating immature lobuli show proliferation within the fat pad where AQP3 expression is seen in the periphery of the islet (*arrows*). The *inset* shows the confocal view of the area indicated by a *rectangle*. A projection image of consecutive 2-slice confocal images at 0.5-μm intervals for AQP3. Labeling for AQP3 is restricted to the basal and lateral side. Bars, 100 μm and 10 μm in inset

What is the role of AQP3 in the mammary gland? AQP3 has the unique feature that it is permeable by glycerol as well as water and seems to play a role in the transfer of water and/or glycerol from the interstitial fluid into the secretory epithelial cells through the basolateral membrane. Since water and glycerol are essential for the synthesis and secretion of milk, AQP3 may serve as a channel for both. In the lactating rat, significant amounts of glycerol are required to produce milk triglycerides (for review, see Garton 1963). Although the majority of the glycerol carbon of milk triglycerides seems to be derived from plasma glucose (for review, see Garton 1963), plasma glycerol may be taken up via AQP3 and incorporated directly into milk triglycerides. The presence of AQP3 in some intralobular and interlobular ducts suggests that the duct cells also participate in the secretion of milk.

The expression of AQP3 in the main duct suggests additional roles for this protein. In the main duct near the orifice in the nipple, in particular, AQP3 is present in the basal and intermediate layers of the stratified epithelium, as seen in the epidermis. We previously examined the immunolocalization of AQP3 in various epithelia such as the urinary tract, digestive tract, and respiratory tract (Matsuzaki et al. 1999b). We showed that in these epithelia, AQP3 is expressed on the basal side, as in the epidermis, in the vicinity of the opening to the body surface. We suggested that the role of AQP3 is to maintain the water content of the epithelial cells by supplying water from the basal side. Studies on AQP3-knockout mice showed that epidermal AQP3 is essential to maintain the water content of the skin and prevent dry skin. The AQP3 in the main duct near the orifice may have roles similar to the AQP3 in epithelia, that is, to keep the duct cells hydrated.

In RT-PCR, a relatively clear band for AQP7 and very weak bands for AQP4, AQP5, and AQP9 were also detected. The band for AQP7 may have originated from fat cells within the mammary gland; the expression of AQP7 in fat cells has been described previously (Kishida et al. 2000). We performed immunohistochemistry using antibodies to AQP7 but did not detect AQP7 in the mammary gland including fat cells (T. Matsuzaki et al., unpublished data). At the beginning of this study, we predicted the presence of AQP5 in the apical membrane of the secretory cell, as is commonly seen in glands such as the salivary, lacrimal, and sweat glands (Matsuzaki et al. 1999a, 2003). However, AQP5 was not detected immunohistochemically in the mammary gland. We also raised antibodies to AQP2 (Tajika et al. 2002), AQP4, AQP6, and AQP9 and performed immunohistochemistry. There was no detectable labeling for these isoforms. Supposing that the transfer of water through the alveolar epithelium occurs transcellularly, it is predicted that the apical membrane bears aquaporin(s). How does water transfer through the apical membrane occur in milk secretion? One possibility is that there is a new aquaporin isoform yet to be identified in the apical membrane. The other possibility is that the transfer requires no aquaporin water channel. Water transfer can occur via other channels and transporters such as sugar transporters (Loo et al. 1996) and by simple diffusion

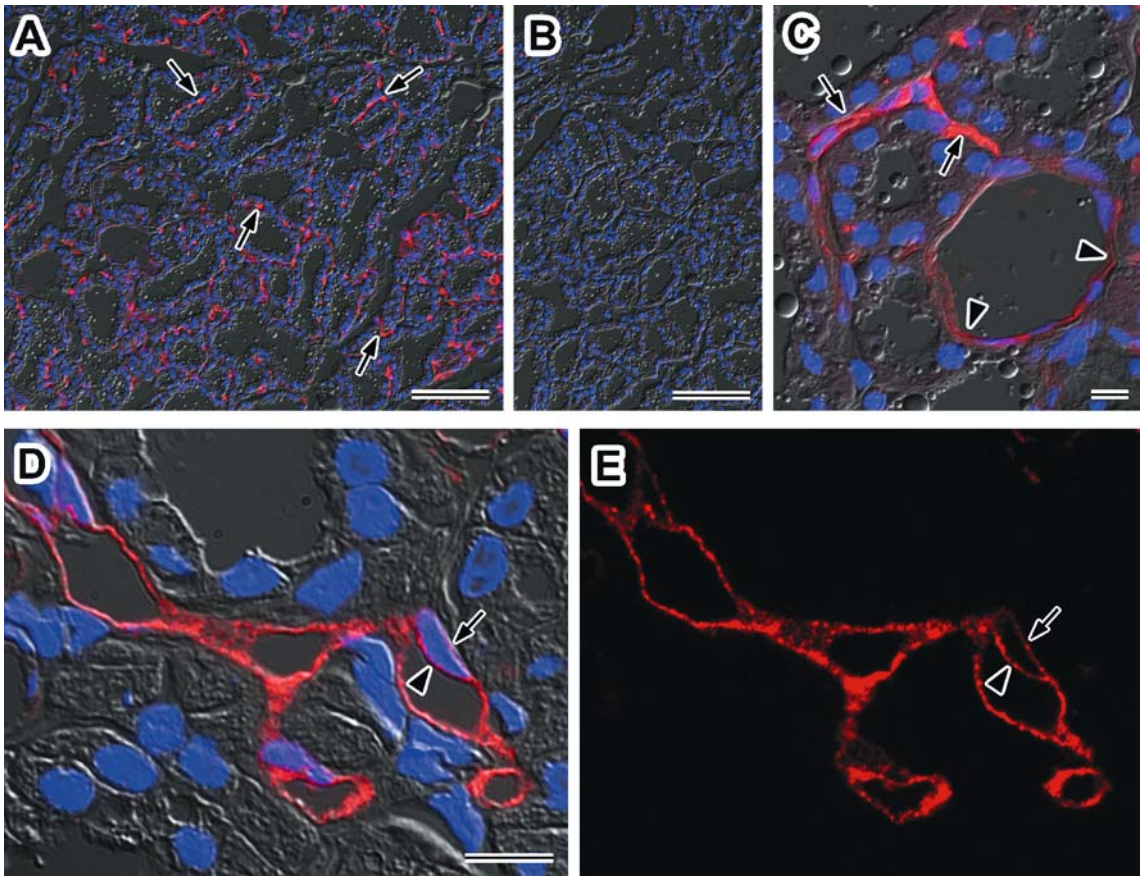

Fig. 6 Immunofluorescence microscopy of aquaporin-1 (AQP1) in the lactating rat mammary gland. Cryostat sections (**A–C**) and a semithin frozen section (**D, E**) were stained. AQP1 detected by the use of GPTM31 (**A, B**) or AffRaTM31 (**C–E**) was labeled with Rhodamine Red-X (*red*). Nuclei were counterstained with DAPI (*blue*). Fluorescence images for AQP1 and nuclei merged with corresponding Nomarski images are shown (**A–D**). **A** A lower magnification view: Labeling for AQP1 is scattered in the stroma (*arrows*) but not in the alveolar epithelium. **B** A section was incubated with GPTM31 in the presence of TM31 peptide (20 μg/ml) used as an immunogen. No labeling is seen. **C** A higher magnification view: Labeling for AQP1 is present in capillaries (*arrows*) and venules (*arrowheads*). **D, E** A higher magnification view of capillaries: A fluorescence image for AQP3 alone is shown in **E**. Labeling for AQP1 is present in both the apical (*arrowhead*) and basolateral (*arrow*) membranes. Bars in **A, B**, 100 μm and in **C, D**, 10 μm

Fig. 7 Changes in the expression of aquaporin-1 (AQP1) during development. Resting-phase mammary gland from a 6-week-old virgin female rat (**A**) and pregnant-phase mammary gland from a pregnant rat on day 17 post coitum (**B**). Cryostat sections were stained. AQP1 detected by the use of AffRaTM31 was labeled with Rhodamine Red-X (*red*). Nuclei were counterstained with DAPI (*blue*). Fluorescence images for AQP1 and nuclei merged with corresponding Nomarski images are shown. **A** Epithelial ducts (*asterisks*) infiltrate through a mammary fat pad, and labeling for AQP1 is seen in the capillaries (*arrows*). **B** Differentiating immature lobuli show proliferation within the fat pad. Labeling for AQP1 is seen in the capillaries (*arrows*) and venules (*arrowheads*). Bars, 100 μm

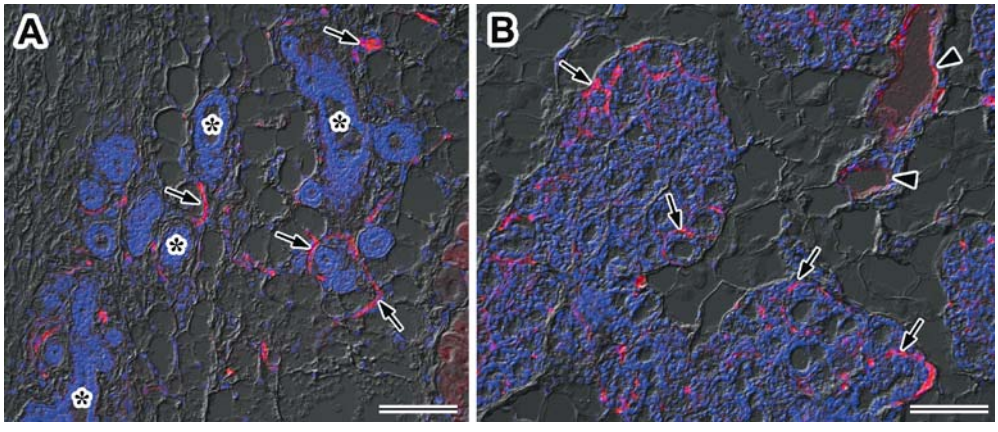

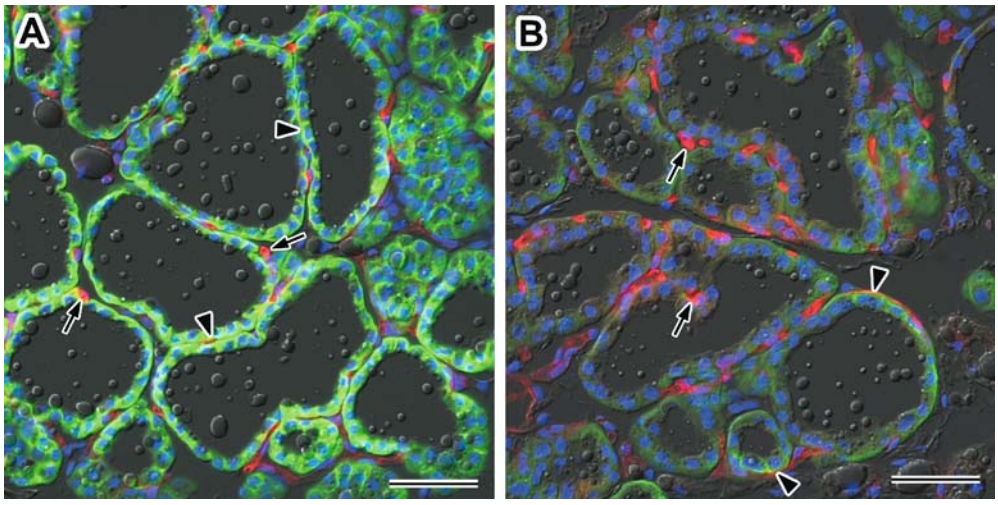

Fig. 8 Immunofluorescence microscopy of aquaporin-1 (AQP1) and AQP3 in the lactating mouse mammary gland. Cryostat sections from a lactating rat on day 8 post partum (**A**) and a lactating mouse on day 7 post partum (**B**). AQP1 and AQP3 were double stained with AffRaTM31 (AQP1) labeled with Rhodamine Red-X (*red*) and AffGPTM5b (AQP3) labeled with FITC (*green*). Nuclei were counterstained with DAPI (*blue*). Fluorescence images for AQP1, AQP3, and nuclei merged with corresponding Nomarski images are shown. Both specimens were processed under exactly the same conditions. Images were captured and processed under the same conditions. Labeling for AQP1 and AQP3 is also present in the mouse mammary gland (**B**), as seen in the rat (**A**). Labeling for AQP1 is localized to the capillaries (*arrows*). Labeling for AQP3 is localized to the basolateral membrane of the alveolar secretory cell (*arrowheads*). The labeling intensity for AQP3 is weaker in the mouse than the rat. Bars, 50 μm

although aquaporin water channels transfer bulk water very rapidly. Because saliva, tears, and sweat are rapidly secreted from acinar cells into the lumen in response to several stimuli, rapid bulk water flow across the apical membrane of acinar cells is necessary. In these glands, AQP5 is located at the acinar cell's apical membrane and serves to rapidly transfer water (Matsuzaki et al. 1999a, 2003). In comparison, milk is secreted gradually, accumulated in the lumen of alveoli and ducts, and excreted rapidly out of the orifice by the contraction of myoepithelial cells encircling acinar cells and duct cells when the milk ejection reflex occurs. Therefore, it seems that rapid bulk water transfer is unnecessary in the apical membrane of the mammary gland acinar cells and does not necessarily require aquaporin water channels.

In summary, we demonstrated the presence of AQP1 and AQP3 in the mammary gland. AQP1 is distributed in both the apical and basolateral membranes of endothelial cells of capillaries and venules and seems to play a role in the transfer of water from the blood to the interstitial space. AQP3 is located at the basolateral membrane of the alveolar and duct epithelial cells and seems to play a role in the transfer of water and/or glycerol from the interstitial fluid to the cytoplasm. These aquaporins seem to participate in the production of milk.

Acknowledgements We thank Y. Takahashi-Tajika and M. Kusama for assistance. This work was supported in part by Grants-in-aid for Scientific Research from the Ministry of Education, Culture, Science and Technology of Japan, and by a scientific grant from the Kazato Research Foundation.

References

Agre P, Sasaki S, Chrispeels MJ (1993) Aquaporins: a family of water channel proteins. Am J Physiol Renal Physiol 265:F461

Agre P, King LS, Yasui M, Guggino WB, Ottersen OP, Fujiyoshi Y, Engel A, Nielsen S (2002) Aquaporin water channels—from atomic structure to clinical medicine. J Physiol (Lond) 542:3–16

Fushimi K, Uchida S, Hara Y, Hirata Y, Marumo F, Sasaki S (1993) Cloning and expression of apical membrane water channel of rat kidney collecting tubule. Nature 361:549–552

Garton GA (1963) The composition and biosynthesis of milk lipids. J Lipid Res 4:237–254

Ishibashi K, Sasaki S, Fushimi K, Yamamoto T, Kuwahara M, Marumo F (1997) Immunolocalization and effect of dehydration on AQP3, a basolateral water channel of kidney collecting ducts. Am J Physiol Renal Physiol 272:235–241

Kishida K, Kuriyama H, Funahashi T, Shimomura I, Kihara S, Ouchi N, Nishida M, Nishizawa H, Matsuda M, Takahashi M, Hotta K, Nakamura T, Yamashita S, Tochino Y, Matsuzawa Y (2000) Aquaporin adipose, a putative glycerol channel in adipocytes. J Biol Chem 275:20896–20902

Loo DDF, Zeuthen T, Chandy G, Wright EM (1996) Cotransport of water by the Na^+/glucose cotransporter. Proc Natl Acad Sci USA 93:13367–13370

Ma T, Song Y, Yang B, Gillespie A, Carlson EJ, Epstein CJ, Verkman AS (2000) Nephrogenic diabetes insipidus in mice lacking aquaporin-3 water channels. Proc Natl Acad Sci USA 97:4386–4391

Matsuzaki T, Suzuki T, Koyama H, Tanaka S, Takata K (1999a) Aquaporin-5 (AQP5), a water channel protein, in the rat salivary and lacrimal glands: immunolocalization and effect of secretory stimulation. Cell Tissue Res 295:513–521

Matsuzaki T, Suzuki T, Koyama H, Tanaka S, Takata K (1999b) Water channel protein AQP3 is present in epithelia exposed to the environment of possible water loss. J Histochem Cytochem 47:1275–1286

Matsuzaki T, Tajika Y, Suzuki T, Aoki T, Hagiwara H, Takata K (2003) Immunolocalization of water channel, aquaporin-5 (AQP5) in the rat digestive system. Arch Histol Cytol 66:307–315

Nejsum LN, Kwon T-H, Jensen UB, Fumagalli O, Frøkiær J, Krane CM, Menon AG, King LS, Agre PC, Nielsen S (2002) Functional requirement of aquaporin-5 in plasma membranes of sweat glands. Proc Natl Acad Sci USA 99:511–516

Nielsen S, Smith BL, Christensen EI, Agre P (1993) Distribution of the aquaporin CHIP in secretory and resorptive epithelia and capillary endothelia. Proc Natl Acad Sci USA 90:7275–7279

Nielsen S, Frøkiær J, Marples D, Kwon T-H, Agre P, Knepper MA (2002) Aquaporins in the kidney: from molecules to medicine. Physiol Rev 82:205–244

Preston GM, Carroll TP, Guggino WB, Agre P (1992) Appearance of water channels in *Xenopus* Oocytes expressing red cell CHIP28 protein. Science 256:385–387

Sabolić I, Valenti G, Verbavatz JM, Van Hoek AN, Verkman AS, Ausiello DA, Brown D (1992) Localization of the CHIP28 water channel in rat kidney. Am J Physiol Cell Physiol 263:1225–1233

Shennan DB, Peaker M (2000) Transport of milk constituents by the mammary gland. Physiol Rev 80:925–951

Shin BC, Suzuki T, Tanaka S, Kuraoka A, Shibata Y, Takata K (1996) Connexin 43 and the glucose transporter, GLUT1, in the ciliary body of the rat. Histochem Cell Biol 106:209–214

Smith BL, Agre P (1991) Erythrocyte M_r 28,000 transmembrane protein exists as a multisubunit oligomer similar to channel proteins. J Biol Chem 266:6407–6415

Song Y, Sonawane N, Verkman AS (2002) Localization of aquaporin-5 in sweat glands and functional analysis using knockout mice. J Physiol 541:561–568

Tajika Y, Matsuzaki T, Suzuki T, Aoki T, Hagiwara H, Tanaka S, Kominami E, Takata K (2002) Immunohistochemical characterization of the intracellular pool of water channel aquaporin-2 in the rat kidney. Anat Sci Int 77:189–195

Takata K, Fujikura K, Suzuki M, Suzuki T, Hirano H (1997) GLUT1 glucose transporter in the lactating mammary gland in the rat. Acta Histochem Cytochem 30:623–628

Takata K, Matsuzaki T, Tajika Y (2004) Aquaporins: water channel proteins of the cell membrane. Prog Histochem Cytochem 39:1–83

Zhang R, Skach W, Hasegawa H, Van Hoek AN, Verkman AS (1993) Cloning, functional analysis and cell localization of a kidney proximal tubule water transporter homologous to CHIP28. J Cell Biol 120:359–369